INDIAN JOURNAL OF SCIENCE AND TECHNOLOGY

ORIGINAL ARTICLE

Check for updates

OPEN ACCESS

Received: 28/04/2026

Accepted: 07/05/2026

Published: 09/06/2026

Citation: Giri S, Autee A, Kadam A, Khansole A (2026) Atomic Force Microscopic Investigations of Improved Wetting Behavior of the Graphene Coated Copper Substrate by Novel Spray Coating Method. Indian Journal of Science and Technology 19(20): 1384-1396. https ://doi.org/10.17485/IJST/v19i20.686

Corresponding author.

sudhavgiri@gmail.com

Funding: None

Competing Interests: None

Copyright: © 2026 Giri et al. This is an open access article distributed under the terms of the Creative Commons Attribution License, which permits unrestricted use, distribution, and reproduction in any medium, provided the original author and source are credited.

Published By Indian Society for Education and Environment (iSee)

ISSN
Print: 0974-6846
Electronic: 0974-5645

Atomic Force Microscopic Investigations of Improved Wetting Behavior of the Graphene Coated Copper Substrate by Novel Spray Coating Method

Sudhakar Giri[1,2]*, Arun Autee[4], Abhijeet Kadam[3], Ankush Khansole[2]

1 Dr. Babasaheb Ambedkar Marathwada University Chh. Sambhajinagar, India
2 Department of Mechanical Engineering, CSMSS, Chh. Shahu College of Engineering, Chhattrapati Sambhajinagar - 431011, India
3 Department of Physics, CSMSS, Chh. Shahu College of Engineering, Chhattrapati Sambhajinagar - 431011, India
4 Department of Mechanical Engineering, Maharashtra Institute of Technology Chhattrapati Sambhajinagar - 431011, India

Abstract

Objectives: To perform and analyze the characterization of graphene and its coating on a copper substrate, and to investigate the improvement in the wetting behavior of the coated copper substrate through a morphological study after graphene coating. **Method:** Graphene was characterized by XRD, Raman spectroscopy, and SEM before preparing the xylene and IPA-assisted colloidal spray solution. This spray solution was used to coat a 2 mm-thick, 25.4 mm-diameter copper disc. The coated metal disc was further characterized by XRD, Raman spectroscopy, AFM, and contact angle measurements. **Findings:** Advanced characterization techniques revealed the full spectral profile of graphene. The number of graphene layers calculated from XRD analysis is 5-6, indicating the use of a few-layer graphene sample in this study. D, G, and 2D band have peaks at 1357 cm^{-1}, 1593 cm^{-1}, and 2670 cm^{-1}, respectively. SEM and AFM studies revealed the surface morphology of the graphene coating on the copper substrate. The wettability behavior of the bare Cu surface and the graphene-coated Cu (Gr@Cu) surface was examined. For the bare Cu surface, the contact angles were measured, yielding an average of approximately 93°, indicating a slightly hydrophobic nature. In contrast, the Gr@Cu surface exhibited significantly higher contact angles, with an average of about 104°, indicating enhanced hydrophobic behavior. This increase in contact angle after graphene coating is attributed to the unique surface morphology of graphene sheets, which introduces micro- and nanoscale roughness and lowers surface energy. Contact angle measurements indicated a shift in the surface's wetting behavior. These findings are useful for promoting drop-wise condensation in heat exchangers. **Novelty:** This study demonstrates the application of a simple, mass-scalable, in-situ solution spray-coating method for the surface functionalization of metal substrates and investigates wetting insights after surface functionalization using AFM.

Keywords: Graphene; Heat exchanger; spray coating; Xylene; hydrophobic; AFM

1 Introduction

Different coatings are applied on metal substrates to inhibit corrosion. Most often, various paints are applied to protect the underlying metal surfaces. However, for heat exchanger metal substrates, different coating materials are needed, as the applied coating should not compromise thermal performance. Therefore, there is a need to explore new conductive coating materials and corrosion inhibitors[1],[2]. Different methods are used to improve the performance of heat exchangers that use solid particles with high thermal conductivity to increase heat transfer between fluids[3]. Graphene, considered a wonder material of the century, is an ideal candidate for coating metal substrates used in heat exchangers due to its intrinsic physical properties. Graphene and its derivatives are applied to various conductive and non-conductive substrates by using various techniques[4]. However, the stability of graphene film is still under study, and therefore, the properties of graphene are not fully explored. Hydrophobicity is of importance in phase change heat transfer as it promotes DWC (drop-wise condensation)[5]. Preston D. et al[5] investigated the potential of graphene coating to promote DWC. A graphene coating deposited by CVD (Chemical vapor deposition) on copper substrates demonstrated 4x greater heat transfer enhancement than uncoated copper tubes. Shaikh K. et al.[6] demonstrated that applied zirconium coating retarded fouling with enhanced heat transfer of the SS316L grade heat exchanger surface. Various studies[7],[8],[9] demonstrated the potential of graphene coating to improve heat exchanger performance. Khose et al.[8],[9] investigated the performance of a graphene-coated heat exchanger by using CFD analysis. Their CFD analysis demonstrated improvements in thermal performance parameters; however, achieving the reported graphene coating thickness with current coating methods is difficult.

Various Characterization techniques, including XRD (X-ray Diffraction)[10], Raman spectroscopy[11],[12], FTIR (Fourier Transform Infrared Spectroscopy)[13], AFM (Atomic Force Microscopy)[14],[15],[16] used to characterize graphene and its derivatives. These advanced characterization techniques, including SEM (Scanning Electron Microscopy) and TEM (Transmission Electron Microscopy) reveal crystallinity, the number of graphene layers, various functional groups, and surface morphology.

There are conflicting reports about the wettability of graphene and graphene-coated copper substrates[4]. Yusuf A et al.[3] noted that the contact angle measurement method should be complemented with other surface-morphology analysis techniques, such as AFM and SEM images, to understand the shift in wetting behavior when graphene is used for surface functionalization. They advocated the significant advantage of AFM studies for understanding the wettability of graphene-coated substrates. Kim et al.[17] investigated the effects of graphene layers and the ambient environment. Their investigation shows that the water contact angle increases from 85.9° to 90.6° as the number of graphene layers increases from 0 to 6 on a copper substrate. Variable exposure duration to environmental conditions also significantly affects wettability[17]. Belyaeva et al.[18] investigated the wettability of a copper substrate coated with graphene by CVD to understand the effects of substrate crystallinity and the deposition method. The reported water contact angle indicates that the copper substrate becomes slightly hydrophobic after graphene deposition, transforming from a hydrophilic surface. In summary, due to greater disagreement across reported studies on the wetting behavior of graphene and graphene-deposited substrates, the following research gaps are identified. There is a need for a simple, mass-scalable method for depositing or coating graphene on metal substrates. There is also a need to investigate the effect of surface morphology to understand the underlying mechanism behind changes in wetting behavior.

Liu Z et al.[19] were the first to report a xylene-based dispersion of graphene in aromatic petroleum resin using a solution-mixing method and studied the effect of xylene content on dispersion quality. The obtained graphene dispersion solution was then used to coat 2024-grade aluminum alloy plates to investigate their corrosion protection performance. Graphene with epoxy binders for coatings was reported in some of the available literature. However, when hardener is added, the agglomeration of graphene in the base solvent with resin is one of the major hurdles in preparing a sustainable spray solution for mechanical applications on metal substrates. The spray coating method, which is ideal for uniform thin coatings, requires a thinner spray solution than other methods. In this work, we demonstrated successful coating of graphene on a copper surface by xylene-assisted physical grafting using a simple, mass-scalable coating method to modify wettability, as confirmed by various characterization techniques.

This study demonstrates the coating of a copper substrate with graphene using a simple, mass-scalable solution spray-coating method. The bare and coated copper substrate was then subjected to various characterization techniques. After confirming the deposition of graphene on a copper substrate via spectral analysis, thermal characterization was performed to evaluate its potential for thermal management applications. CAM (Contact angle measurement) using the sessile drop method to explore wetting behavior is a particularly useful technique for condensation heat transfer analysis. The more hydrophobic the surface, the greater the DWC due to the surface-morphology effect of the applied coating. In this study, it is found that the hydrophobic behavior of the coated copper substrate improved compared with that of the bare, uncoated copper surface. Therefore, to understand the underlying mechanism of the improvement in water contact angle post-coating, it was necessary to conduct

surface morphological investigations using SEM/EDS and AFM. AFM study revealed nanoscale surface morphology, thereby exploring the 'Cassie-Baxter' effect. These findings are useful for controlling surface functionalization of heat exchanger metal surfaces, particularly using DWC heat transfer. This study used a simple, mass-scalable, in-situ solution spray-coating method, in contrast to other methods that are either energy-intensive or require specialized technology to deposit graphene on substrates. Further, CAM demonstrated improved wetting behavior in the heat exchanger application, thereby promoting DWC. To the best of the authors' knowledge, this is the first study to investigate the wetting behavior of the coated copper substrate when xylene is used as the dispersion agent in the synthesis of a graphene spray solution.

The novelty of the present work is summarized as follows. This study demonstrates a simple, scalable graphene spray-coating method for surface functionalization of copper substrates and provides clear insights into the relationship between surface morphology and the wettability of graphene-coated Cu surfaces.

2 Methodology

2.1 Materials

Commercial graphene powder, synthesized via an enhanced oxidative exfoliation (modified Hummer's method) and obtained from a commercial source (KNV Incorporation, Nagpur), was used in this investigation. Although this synthesis route can introduce structural defects and surface oxygen groups, it remains one of the most reliable and scalable approaches for producing graphene-based materials suitable for engineering applications. Before preparing the coating formulation, the as-received graphene was characterized by diffraction, vibrational spectroscopy, and electron microscopy to confirm its crystalline nature, layered structure, and chemical identity. After verification, the graphene was dispersed in an organic medium to prepare a sprayable suspension; however, the exact solvent composition and dispersion procedure remain confidential due to proprietary restrictions. The synthesized graphene powder was dispersed in a solvent mixture of xylene and IPA (isopropanol) containing 2% binder, 1% suspension agent, and 3% dispersion agent to prepare a homogeneous suspension with a graphene concentration of 3.96% wt/V. The mixture was initially stirred using a mechanical mixer at 75 rpm to ensure proper blending of all components. Subsequently, the dispersion was ultrasonicated for 15 hours to achieve a highly stable, uniformly dispersed graphene colloidal solution.

Circular specimens were produced from 2 mm-thick copper plates using precision laser cutting, followed by edge finishing and sequential cleaning with a mild detergent, gentle abrasion, and an acetone wash to eliminate impurities and improve surface cleanliness. The graphene film was deposited by spray application inside a controlled chamber to prevent environmental contamination. Each disc was positioned vertically and coated with a short spray burst from a fixed distance of approximately 20 cm, allowing the formation of a thin, uniform layer. The coated specimens were then left undisturbed under ambient laboratory conditions ($\approx$35 °C, 40% RH) for about 30 minutes to ensure proper drying and adhesion.

2.2 Methods of Characterization Techniques

The structural and surface properties of the samples were examined using multiple techniques. Post-deposition analysis was performed using scanning electron microscopy combined with energy-dispersive spectroscopy to observe surface morphology and elemental composition. Prior to imaging, a thin conductive layer was sputtered on the coated samples to improve electron beam interaction and image clarity. Phase and structural features of the deposited graphene were further examined via X-ray diffraction and Raman spectroscopy while carefully controlling laser intensity to avoid local heating. Additionally, graphene films were also fabricated on glass slides through drop-casting and spin-assisted spreading from a diluted aqueous dispersion to obtain clearer Raman signals and facilitate microscopic examination of film uniformity.

XRD (Bruker, D8 Advanced, Cu Kα radiation, λ = 1.5406 Å) was employed to determine crystal structure, lattice parameters, and interplanar spacing. Fourier Transform Infrared Spectroscopy (FTIR-Shimadzu) confirmed the presence of characteristic functional groups. Raman spectroscopy (Xplora plus, Horiba, France, with excitation frequency of 532 nm, 1200 nm grit/mm) was used to assess the quality and defect density of graphene. Field Emission Scanning Electron Microscopy (FESEM/EDS- JEOL/Oxford Inca) and Atomic Force Microscopy (AFM) analyzed surface morphology and roughness. Contact angle measurements were performed to evaluate surface wettability, which is critical for understanding heat transfer and anti-fouling behavior in heat exchanger applications.

2.3 Validation of the Experimental Data

The experimental data obtained by XRD were compared with the standard ICSD cards shown in Figure 1. A standard silicon wafer was used to calibrate the Raman shifts with the Raman spectra of the present study. Also, graphs plotted using Raman

spectroscopic data were compared with available standard graphs from the literature, cited at the appropriate place in the following sections. SEM and AFM images of graphene, bare, and coated copper substrates in this study were compared and analyzed using the latest relevant literature in this domain.

3 Results and Discussion

3.1 XRD and Spectroscopic Characterization

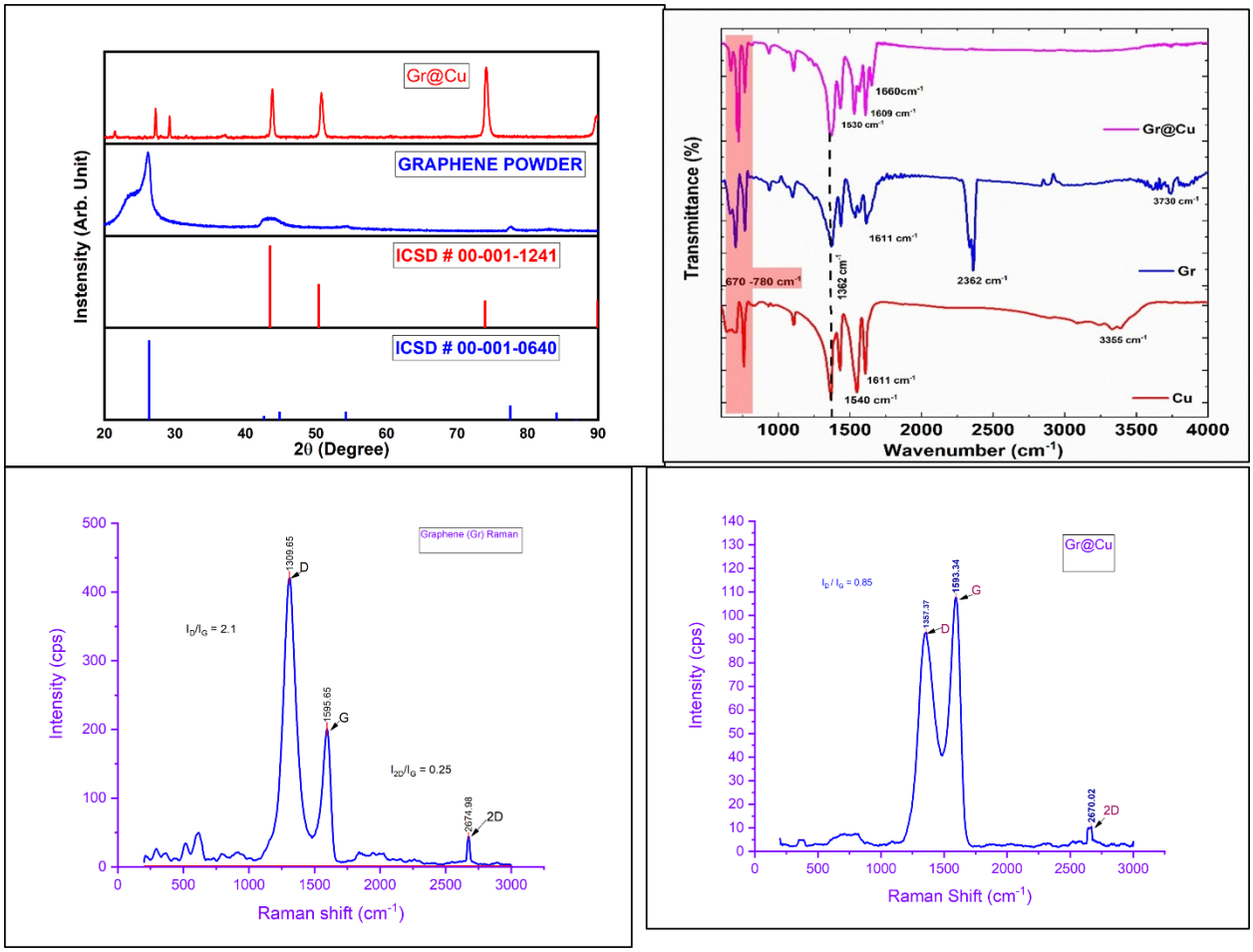


Fig 1. (a) XRD patterns of graphene powder and spray-coated film on copper substrate compared with standard ICSD reference data **(b)** FTIR of graphene powder **(c)** Raman spectroscopy of graphene powder **(d)** Raman spectroscopy of graphene deposited on copper substrate through spray coating. ** Please refer appendices for individual image.

The **XRD analysis** shown in Figure 1(a) revealed the successful formation of crystalline graphene layers over metallic copper, with characteristic diffraction peaks corresponding to Cu (111) and (200) planes [20], and an additional broad peak near $2\theta \approx 26.4^{\circ}$, confirming the presence of few-layer graphene. The **FTIR spectra** of Cu, Gr, and Gr@Cu samples in Figure (b) provide valuable insights into their surface functional groups, interfacial bonding, and chemical interactions (13) influencing heat transfer properties.

Raman spectroscopy [12] has emerged as a non-destructive, versatile, and inevitable advanced characterization technique in the analysis of carbon-based materials. Table 1 summarizes the Raman spectroscopic analysis of graphene and a graphene spray solution synthesized using xylene and IPA. This solution was used to coat a copper substrate for graphene deposition via spray coating.

Table 1. Comparison of the D, G, and 2D band positions in Raman spectra across the present and latest studies.

Sr. No	Reference	Graphene synthesis Method	Graphene Coating method	Band Positions (cm-1)		
				D	G	2D
1	Ott et al.[12]	Comparative review	MC[1], CVD[2], LPE[3]	1350	1580	2700
2	Liu et al.[19]	Chemical exfoliation	Surface Coating	—	1576	—-
3	Yamagishi et al.[21]	Cedar wood carbonization	Powder sample analyzed	1350	1590	2690
4	Low et al.[22]	Chemical exfoliation	Spin-Coating	1334	1578	2679
5	ThermoFisher Application Note No. **AN53174****	NA	NA	1350	1582	2682
6	**Present work**	**Chemical exfoliation (Gr used)**	**Spin coating**	**1310**	**1596**	**2675**
		Gr@Cu	**Spray Coating**	**1357**	**1593**	**2670**

** Please refer appendix, [1]Micromechanical cleavage (MC), [2]Chemical vapor deposition (CVD), [3]Liquid phase exfoliation (LPE)

Raman spectra analysis of the present work in comparison with[12],[19],[21],[22] indicates that the present work used a few layers of graphene as a raw material, mixed with xylene and IPA to prepare a graphene spray solution. Further Raman spectra of Gr@Cu show that graphene was well dispersed in the spray solution and deposited on the copper substrate.

Intercalation and steric hindrance effect of xylene between graphene layers[19], further helped to reduce the defects, which is evident from the comparatively less intense D peak than the G peak. This proves that xylene can be used as an effective dispersion agent to prepare a stable sprayable graphene spray solution, which is in agreement with Liu Z et al[19]. These findings can open the opportunity for a mass-scalable graphene coating process on heat exchanger materials in efficient and effective energy management.

In Raman spectroscopic analysis of graphene powder, all three aforementioned characteristic bands appeared at their prominent positions. As displayed in Figure 1(c) D, G, and 2D band has peaks at 1310 cm^{-1}, 1596 cm^{-1} and 2675 cm^{-1}, respectively. The I_D / I_G ratio is 2.1, whereas the I_{2D} / I_G ratio is 0.25, which signifies that the present sample is few-layer graphene, which is supportive of the findings by XRD analysis. The calculated number of layers in XRD analysis is 5-6 from the (002) peak position, which appeared around $2\Theta = 26^{\circ}$. These findings are in very good agreement with the analyses reported in various studies.

In preparation of the xylene-based graphene spray solution, the same Graphene powder is used further. It is evident from Figure 1(d), which shows Raman spectroscopy of the spray-coated Cu substrate, that graphene was dispersed well in the spray solution and deposited uniformly on the substrate. All peaks of different characteristic band positions of Graphene appeared at their prominent wave number positions. As shown in Figure 1(d), D, G, and 2D band have peaks at 1357 cm^{-1}, 1593 $cm^{-1}$and 2670 cm^{-1} , respectively. The I_D / I_G ratio is 0.85, whereas I_{2D} / I_G ratio is 0.1, signifying a degree of reduction in defects. Further, there is scope for future critical analysis of Raman spectroscopy, which is part of a separate investigation.

3.2 Morphological Characterization

3.2.1. Atomic Force Microscopic Analysis

Figures 2(a-c) depict the 2D topographic, 3D surface morphology, and height distribution histogram of the synthesized graphene sample. In Figure 2(a), the two-dimensional AFM image clearly shows a sheet-like layered morphology, characteristic of exfoliated graphene flakes. The surface exhibits uniformly distributed nanosheets with wrinkles and overlapping domains, indicating few-layer graphene stacking[14]. The smooth yet corrugated appearance arises from partially restacked sheets and interfacial voids formed during solvent evaporation in the coating process. Figure 2(b) presents the corresponding 3D AFM image, which highlights the vertical height variations across the graphene surface. The presence of ridge-like elevations and depressions suggests micro-wrinkling typical of flexible graphene nanosheets. Such texture enhances surface area and provides excellent interfacial compatibility for subsequent metallic coating (e.g., Cu), which is essential for improved phonon transfer and heat dissipation. Figure 2(c) shows the height distribution histogram of the same scanned region. The height profile is centered near 0 nm, with a symmetric distribution extending from approximately −80 to +60 nm, confirming that the graphene surface is relatively balanced in its peak-to-valley texture. The sharp central peak indicates a dominant smooth region, while minor tails correspond to deeper valleys and higher ridges.

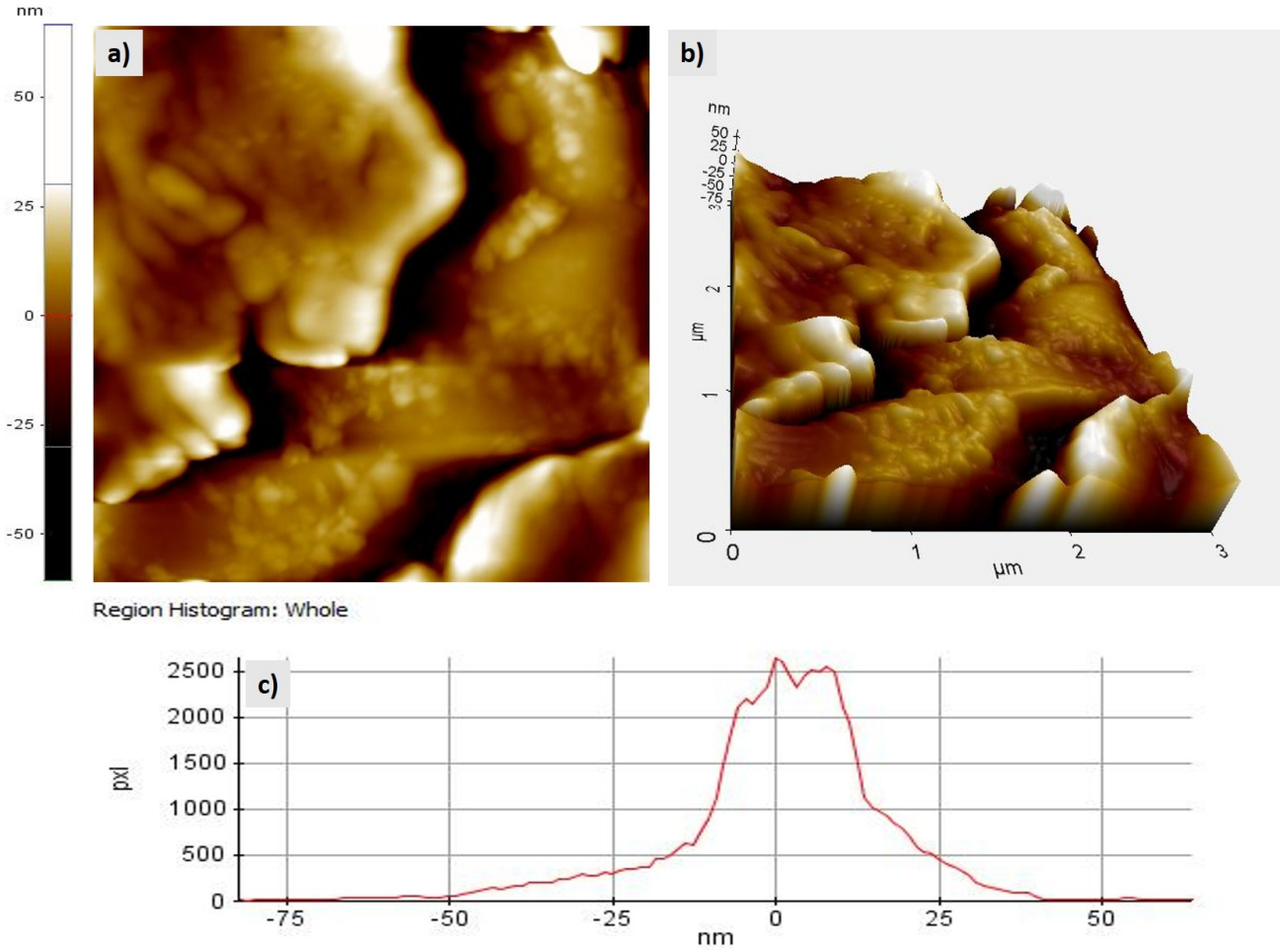


Fig 2. (a) 2D Topography, **(b)** 3D Morphology and **(c)** Histogram profile of Gr.

Table 2. AFM surface roughness parameters of Graphene (Gr) sample

Region	Min (nm)	Max (nm)	Mid (nm)	Mean (nm)	Rpv (nm)	Rq (nm)	Ra (nm)	Rz (nm)	Rsk	Rku
Whole	-83.593	62.366	-10.614	0.000	145.959	15.635	11.285	138.387	0.772	5.158

Quantitatively, the AFM parameters (Table 2) show that the peak-to-valley roughness (Rpv) is 145.959 nm, while the average roughness (Ra) and root mean square roughness (Rq) are 11.285 nm and 15.635 nm, respectively. The skewness (Rsk = 0.772) being positive suggests a dominance of peaks over valleys, whereas the kurtosis (Rku = 5.158) (>3) indicates sharp, well-defined surface features. These results confirm that the graphene sheet surface is moderately rough and highly textured, which enhances wettability, adhesion, and interfacial phonon coupling—critical factors for thermal management and heat exchanger applications.

The two-dimensional AFM image (Figure 3a) of the copper substrate reveals a granular surface morphology consisting of uniformly distributed nanoscale grains. The bright and dark contrasts correspond to surface elevations and depressions, indicating a polycrystalline texture typical of electrodeposited or sputtered Cu films[23]. The grains appear densely packed with slight ridges, signifying a moderately rough surface beneficial for improved graphene adhesion during coating. The three-dimensional AFM image (Figure 3b) further illustrates the topographical variations of the Cu surface. The 3D view shows well-defined hill-like structures with a consistent height distribution, confirming the presence of nanoscale roughness. Such surface asperities enhance the mechanical interlocking and interfacial bonding strength when the graphene layer is deposited, thereby improving overall coating stability and electrical contact quality. The uniformity of the roughness also indicates good control over the deposition or polishing process.

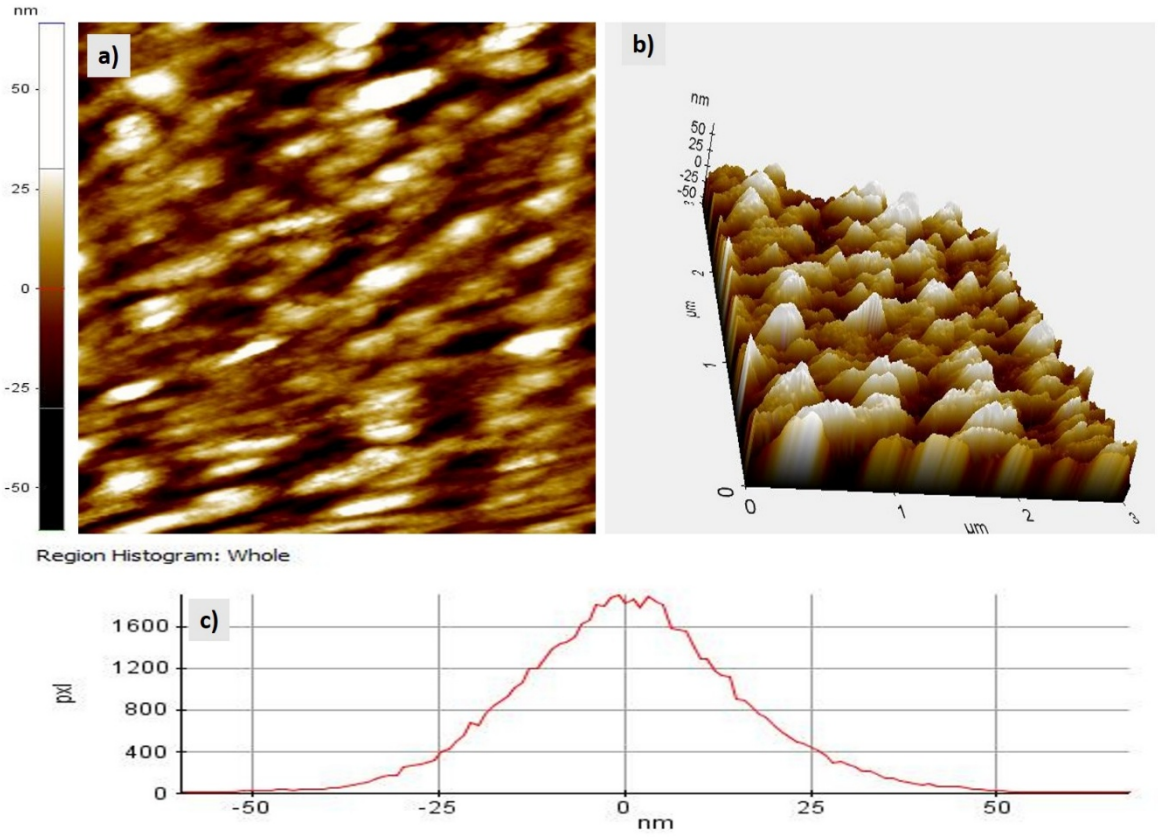


Fig 3. (a) 2D Topography, **(b)** 3D Morphology and **(c)**Table **??**. AFM surface roughness parameters of Cu substrate.

The height distribution histogram (Figure 3c) displays a nearly symmetric bell-shaped curve centered around 0 nm, suggesting a balanced distribution of peaks and valleys. The curve exhibits a narrow width, which indicates that most of the surface lies close to the mean height level, with few extreme deviations [23]. This confirms that the Cu surface has a controlled nanoscale roughness with minimal topographic irregularities.

Table 3. AFM surface roughness parameters of Cu surface

Region	Min (nm)	Max (nm)	Mid (nm)	Mean (nm)	Rpv (nm)	Rq (nm)	Ra (nm)	Rz (nm)	Rsk	Rku
Whole	-60.607	66.628	3.011	0.000	127.235	15.329	11.922	124.520	-0.134	3.528

Quantitatively, the AFM parameters summarized in Table 3 show that the peak-to-valley roughness (Rpv) is 127.235 nm, while the root mean square roughness (Rq) and average roughness (Ra) are 15.329 nm and 11.922 nm, respectively. The slightly negative skewness (Rsk = -0.134) indicates a surface dominated by shallow valleys rather than sharp peaks, while the kurtosis (Rku = 3.528) value close to 3 signifies a relatively normal surface profile. Overall, the Cu substrate exhibits a moderately rough and uniform morphology ideal for graphene deposition and enhanced interfacial coupling in composite structures [24].

The two-dimensional AFM micrograph (Figure 4a) of the Gr@Cu surface exhibits a heterogeneous and granular morphology characterized by randomly distributed bright and dark features. The bright regions correspond to protrusions or Cu-rich domains, while the darker zones represent graphene-covered areas. This pattern indicates the successful deposition of graphene sheets over the Cu substrate, where the sheets form an interconnected network with embedded metallic features. The overall surface appears sheet-like with embedded clusters, suggesting partial coverage and interfacial interaction between graphene and copper [25].

The three-dimensional AFM image (Figure 4b) confirms the topographical complexity of the Gr@Cu surface. The 3D structure displays uneven peaks and valleys, with high ridges corresponding to Cu-rich regions that remain slightly exposed through the graphene layer (14). The vertical scale (approximately $\pm$50 nm) indicates that the surface maintains moderate

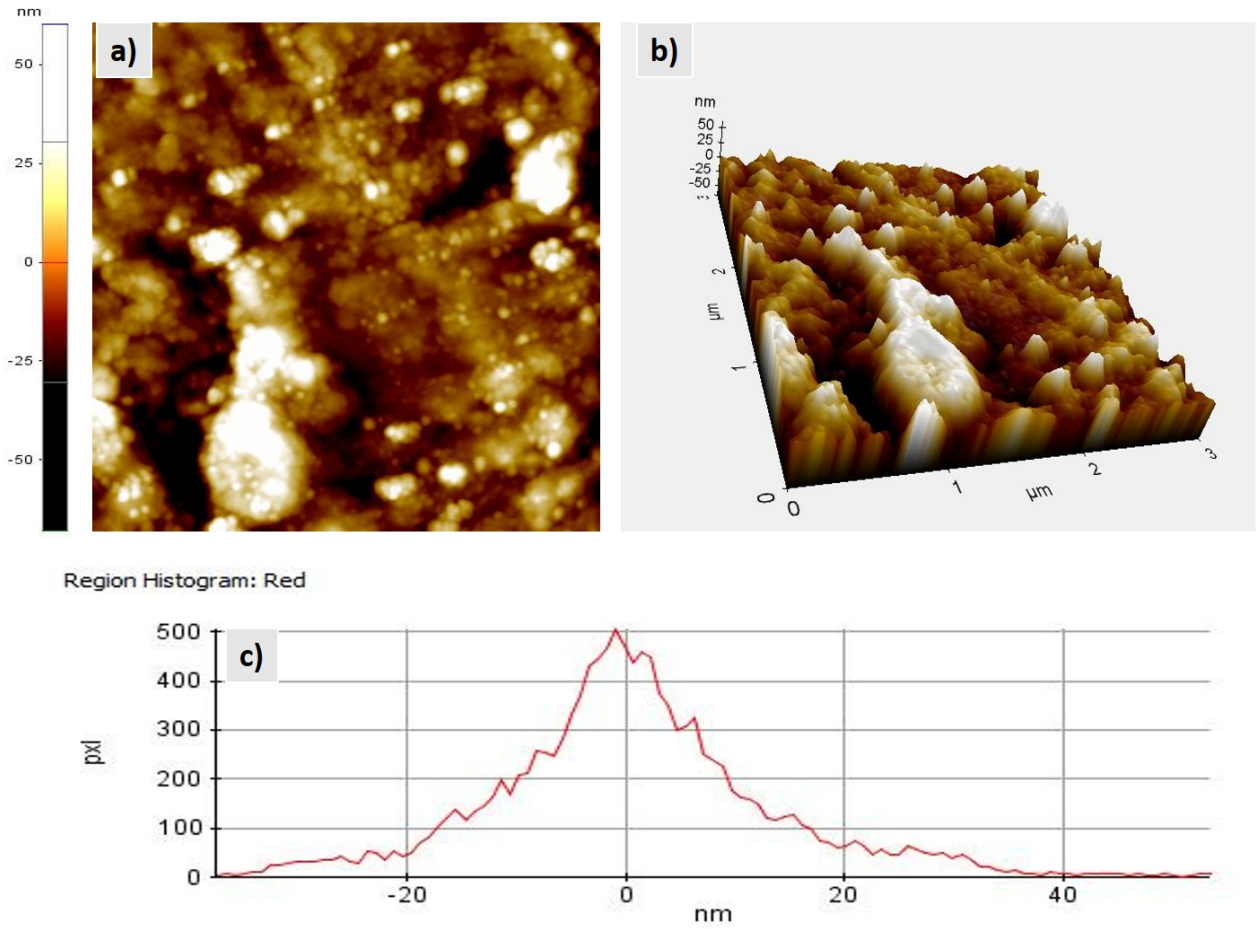


Fig 4. (a) 2D Topography, **(b)** 3D Morphology and **(c)** Histogram profile of Gr@Cu

roughness. This nanoscale topography promotes enhanced surface area and heat transfer efficiency, making the composite ideal for heat exchange and thermal management applications. The intimate contact between the graphene sheets and copper substrate enhances thermal conductivity and interfacial phonon coupling, essential for efficient heat dissipation.

The height distribution histogram (Figure 4c) shows a slightly asymmetric profile centered near zero, with a minor skew toward negative values, reflecting a prevalence of shallow depressions on the surface. The distribution confirms moderate surface roughness with balanced height variation, aligning well with the morphological uniformity seen in (a) and (b). The reduced peak intensity compared to pure Cu indicates the smoothing effect of graphene coating, as graphene sheets tend to fill and bridge surface irregularities on the metal substrate.

Table 4. AFM surface roughness parameters of the Gr@Cu surface

Region	Min (nm)	Max (nm)	Mid (nm)	Mean (nm)	Rpv (nm)	Rq (nm)	Ra (nm)	Rz (nm)	Rsk	Rku
Red	-38.404	52.548	7.072	0.013	90.952	12.451	9.202	88.455	-0.323	4.038

Quantitatively, the roughness parameters summarized in Table 4 reveal that the peak-to-valley height (Rpv) of the Gr@Cu composite is 90.952 nm, while the root mean square roughness (Rq) and average roughness (Ra) are 12.451 nm and 9.202 nm, respectively. The slightly negative skewness (Rsk = -0.323) implies a surface dominated by shallow valleys rather than sharp peaks, consistent with the smoothening action of graphene layers. The kurtosis (Rku = 4.038) suggests a leptokurtic height distribution, meaning a few pronounced features exist but overall roughness remains controlled.

The comparative AFM analysis of Cu, Gr, and Gr@Cu surfaces reveals a clear evolution in surface topography and roughness characteristics as the hybrid structure forms. The bare Cu surface exhibits a relatively high surface roughness with Rpv = 127.235

nm, Rq = 15.329 nm, and Ra = 11.922 nm, reflecting a morphology dominated by distinct granular peaks and valleys due to metallic grain boundaries and micro-oxidized patches. Such high roughness provides good thermal contact potential but limited stability and uniformity for interfacial heat transport. Upon deposition of graphene (Gr) synthesized via the modified Hummer's method and spray-coated from xylene dispersion, the surface morphology becomes sheet-like and smoother, with Rpv = 145.959 nm, Rq = 15.635 nm, and Ra = 11.285 nm. The layered structure of graphene introduces extended flat regions interspersed with wrinkles and folds, reducing localized irregularities while maintaining nanoscale corrugations that favor phonon scattering and high in-plane thermal conductivity. In the Gr@Cu hybrid, roughness decreases moderately to Rpv = 90.952 nm, Rq = 12.451 nm, and Ra = 9.202 nm, accompanied by a near-zero skewness (Rsk = -0.323) and a kurtosis (Rku = 4.038) indicative of a smoother yet structured surface. This reduced roughness and more uniform topography confirm that graphene acts as a surface leveling and conductive coating, filling gaps between Cu asperities and forming an intimate interface that enhances interfacial phonon coupling. The resulting optimized roughness ensures a balance between mechanical anchoring and thermal conduction pathways, significantly improving heat exchange efficiency. In essence, the Cu substrate provides high thermal capacity, graphene contributes superior thermal conductivity, and the composite's controlled roughness minimizes interfacial resistance, making Gr@Cu an ideal material for advanced thermal management and heat exchanger applications.

3.2.2. SEM analysis

The SEM micrographs in Figure 5 provide detailed insight into the surface morphology and structural evolution of the samples. Images (a) and (b) correspond to the Gr@Cu hybrid, revealing a compact and agglomerated structure where graphene sheets are uniformly coated over the Cu surface. The graphene layers appear wrinkled and folded, forming interconnected networks that fill the voids between Cu grains [26]. This coating leads to the formation of a continuous conductive pathway and enhanced surface contact area, which is advantageous for efficient thermal transfer and electron conduction in heat-exchanging systems. The agglomerated morphology suggests strong interfacial interaction between Cu and graphene, ensuring mechanical stability and reduced interfacial thermal resistance. Images (c) and (d) represent the bare Cu surface, which shows a relatively smooth and grain-like morphology with clearly defined boundaries and metallic luster. The Cu surface appears compact but lacks the interconnected nanosheet network observed in the hybrid. The absence of carbonaceous coverage leads to limited phonon coupling and higher interfacial scattering, thereby reducing the overall thermal transfer efficiency compared to the hybrid composite. Images (e) and (f) display the morphology of graphene (Gr) synthesized via the modified Hummers' method. The sheets exhibit thin, wrinkled, and layered structures, typical of exfoliated graphene, with stacked and partially crumpled features. This morphology provides a large surface area and high thermal conductivity, making graphene an ideal coating material for metallic substrates.

The morphological transformation from Cu → Gr → Gr@Cu demonstrates the synergistic combination of both components. While Cu offers a stable, conductive base, graphene contributes extended surface area and high phonon conductivity [27], [28]. The Gr@Cu composite exhibits an optimized surface smoother than bare Cu but with interconnected graphene networks, which minimizes interfacial voids and enhances thermal transport efficiency. The agglomerated yet continuous morphology of Gr@Cu promotes superior heat dissipation and interfacial contact, confirming its suitability for heat exchange and thermal management applications.

3.3 Contact Angle Measurement Analysis for Cu and Gr@Cu Surfaces: -

The wettability behavior of the bare Cu surface and the graphene-coated Cu (Gr@Cu) surface was examined through static water contact angle measurements, as shown in the above images (Figure 6a and 6b). Contact angle measurement is a crucial surface analysis technique used to determine a material's hydrophobic or hydrophilic nature, which directly influences its heat transfer efficiency in thermal exchange systems [5], [29]. The contact angle provides insight into the surface energy and interfacial interactions between the solid surface and liquid medium.

For the bare Cu surface (Figure 6a), the contact angles were measured as 93.2° and 92.7°, giving an average value of approximately 93°, which indicates a slightly hydrophobic nature. The smooth morphology of Cu and the presence of surface oxides contribute to moderate wettability. Such surfaces, while capable of good thermal conduction, may not optimally promote nucleate boiling or efficient fluid spreading during heat exchange due to limited liquid–solid contact area.

In contrast, the Gr@Cu surface exhibited significantly higher contact angles of 105.5° and 101.9°, with an average value around 104°, revealing enhanced hydrophobic behavior. This increase in contact angle after graphene coating is attributed to the unique surface morphology of graphene sheets, which introduces micro- and nanoscale roughness and lowers surface energy. The hierarchical texture formed by graphene layers traps air pockets between the liquid droplet and surface, leading to a composite (Cassie–Baxter type) interface that enhances hydrophobicity.

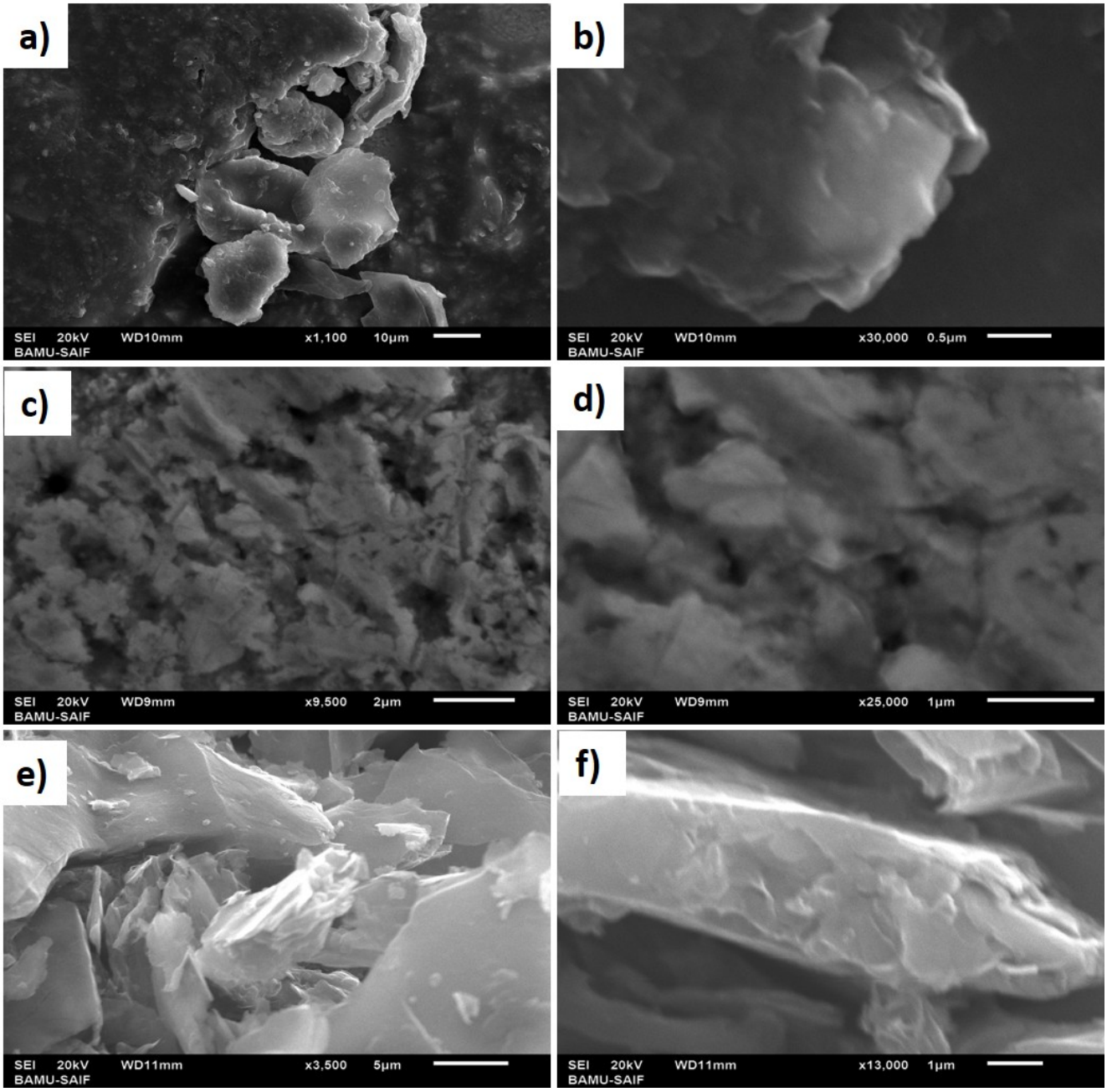


Fig 5. SEM images of (a-b) Gr@Cu, (c-d) Cu and (e-f) Gr

From a heat exchange perspective, this change in surface wetting is particularly valuable. Moderately hydrophobic surfaces like Gr@Cu facilitate better control of condensation and evaporation processes, enabling faster droplet departure and improved thermal transfer cycles. The graphene layer not only increases the thermal conductivity of the Cu substrate but also enhances the durability and corrosion resistance of the surface, thereby maintaining performance over repeated thermal cycles.

4 Conclusion

Thus, this study demonstrates effective use of xylene as a promising dispersion agent for mass scalable spray coating method. Graphene is well dispersed in spray solution. The comprehensive study on the synthesis and characterization of graphene-coated

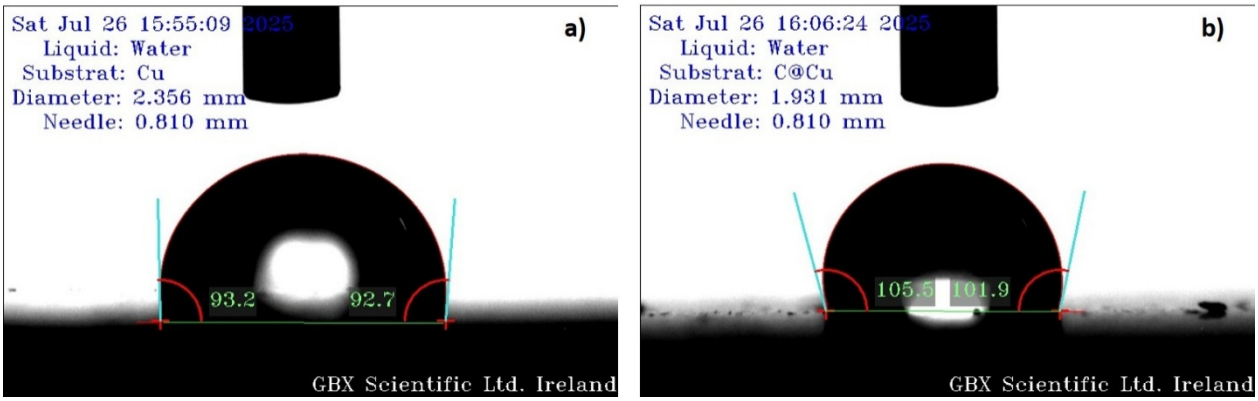


Fig 6. Static water contact angle measurements **(a)** bare copper surface **(b)** Gr@Cu after spray coating.

copper (Gr@Cu) demonstrates a significant improvement in the physicochemical, morphological, and surface properties of Cu after graphene deposition, leading to its potential application in efficient heat-exchanging systems. The XRD analysis revealed the successful formation of crystalline graphene layers over metallic copper, with characteristic diffraction peaks corresponding to Cu (111) and (200) planes, and an additional broad peak near $2\theta \approx 26.4^{\circ}$, confirming the presence of few-layer graphene. SEM micrographs provided clear morphological evidence of graphene coating; pristine Cu exhibited a relatively smooth and dense surface while Gr@Cu showed uniformly distributed wrinkled and layered graphene sheets adhering well to the Cu substrate, in contrast to the exfoliated morphology of pure graphene. The AFM surface analysis further quantified this improvement, showing a considerable enhancement in roughness parameters: the mean roughness (Ra) increased from 5.84 nm for Cu to 9.20 nm for Gr@Cu, while the root mean square roughness (Rq) rose from 7.66 nm to 12.45 nm, and the peak-to-valley height (Rpv) increased from 65.22 nm to 90.95 nm, indicating a more textured surface favorable for fluid interaction and improved thermal boundary contact. The contact angle measurements revealed a shift in surface wettability due to graphene incorporation. The pristine Cu substrate showed a moderate hydrophobic nature with an average contact angle of $\approx 93^{\circ}$, while the Gr@Cu surface exhibited a significantly higher angle of $\approx 104^{\circ}$, confirming enhanced hydrophobicity induced by the graphene layer. This modification plays a crucial role in heat exchanger applications, as it minimizes fluid adhesion and promotes efficient droplet mobility, facilitating rapid condensation and evaporation processes. The overall enhancement in surface roughness and hydrophobicity is synergistically beneficial for improved thermal conduction and anti-corrosion performance, as graphene acts as a high-conductivity barrier protecting Cu from oxidation while maintaining effective heat transfer pathways. Thus, the integration of graphene via the optimized xylene–IPA spray-coating technique not only improved the structural stability and surface morphology of Cu but also endowed it with superior wetting and thermal characteristics, making the Gr@Cu composite a promising and scalable candidate for next-generation heat exchangers and thermal management systems.

5 Acknowledgements

Authors are grateful to the authorities and technical team of RUSA, CFART, Dr. Babasaheb Ambedkar Marathwada University, Maharashtra, India for rendering the testing services and experiment facilities. Authors extend their gratitude to Mr. Sanjeev Sharma (KNV Incorporation, Nagpur) for support in raw material.

6 Declaration of Generative AI and AI-assisted technologies in the writing process

During the preparation of this work, the authors reasonably used AI tools (Research Rabbit/Quillbot/Grammarly) to summarize literature, improve readability, and make grammatical corrections. However, no AI tools/service used to interpret or analyze the results. After using this tool/service, the authors reviewed and edited the content as needed and take full responsibility for the publication's content.

7 Conflict of Interest

The authors declare that they have no known competing financial interests or personal relationships that could have influenced the work reported in this paper.

8 Data availability

Data (experimental XRD and Raman data) will be made available upon reasonable request.

9 Funding Information

The authors declare that they have not received funding for this study from any funding agency.

References

1) Patel A. Heat Exchanger Materials and Coatings: Innovations for Improved Heat Transfer and Durability. *International Journal of Engineering Research and Applications*. 2023;13(9):131–142. https://doi.org/10.9790/9622-1309131142.
2) Oon CS, Kazi SN, Hakimin MA, Abdelrazek AH, Mallah AR, Low FW, et al. Heat transfer and fouling deposition investigation on the titanium coated heat exchanger surface. *Powder Technology*. 2020 Aug;373:671–680. https://doi.org/10.1016/j.powtec.2020.07.010.
3) Marzouk SA, Al-Sood MMA, El-Said EMS, Younes MM, El-Fakharany MK. A comprehensive review of methods of heat transfer enhancement in shell and tube heat exchangers. *Journal of Thermal Analysis and Calorimetry*. 2023;p. 7539–7578. https://doi.org/10.1007/s10973-023-12265-3.
4) Yusuf AO, Muscetta M, AlMahri M, Chiesa M, Palmisano G. Understanding the Wettability of Graphene Coatings: Insights, Measurements, and Implications for Diverse Applications. *ACS Applied Electronic Materials*. 2024. https://doi.org/10.1021/acsaelm.4c01292.
5) Preston DJ, Mafra DL, Miljkovic N, Kong J, Wang EN. Scalable graphene coatings for enhanced condensation heat transfer. *Nano Letters*. 2015 May;15(5):2902–2909. https://doi.org/10.1021/nl504628s; https://pubmed.ncbi.nlm.nih.gov/25826223.
6) Shaikh K, Kazi SN, Zubir MNM, Razak BA, Wong K, Wong YH, et al. Investigation of zirconium (Zr) coated heat exchanger surface for the enhancement of heat transfer and retardation of mineral fouling. *Journal of the Taiwan Institute of Chemical Engineers*. 2023 Dec;153:105246. https://doi.org/10.1016/j.jtice.2023.105246.
7) Zhang Y, Wang S, Zhang W, Ding Y, Cheng M, Mu L, et al. Investigation of the condensation heat-transfer between the wet air and 3-D finned-tube heat exchanger surface with different anti-corrosion coatings. *Experimental Heat Transfer*. 2022;35(4):399–418. https://doi.org/10.1080/08916152.2021.1877371.
8) Khose A, Kolhe S, Deshmukh VN. Investigations on the effect of graphene coating on thermophysical properties of aluminium and mild steel for cross flow heat exchanger. *Materials Today: Proceedings*. 2022 Jan;56:2858–2864. https://doi.org/10.1016/j.matpr.2021.10.166.
9) Kolhe S, Khose A, Deshmukh VN. Comparison of thermal performances between copper and stainless steels on application of graphene coatings. *Materials Today: Proceedings*. 2022;56:2865–2872. https://doi.org/10.1016/j.matpr.2021.10.167.
10) Moseenkov SI, Kuznetsov VL, Zolotarev NA, Kolesov BA, Prosvirin IP, Ishchenko AV, et al. Investigation of Amorphous Carbon in Nanostructured Carbon Materials (A Comparative Study by TEM, XPS, Raman Spectroscopy and XRD). *Materials*. 2023 Feb;16(3). https://doi.org/10.3390/ma16031112.
11) Jorio A, Saito R. Raman spectroscopy for carbon nanotube applications. *Journal of Applied Physics*. 2021;129:21102. https://doi.org/10.1063/5.0030809.
12) Ott AK, Ferrari AC. Raman spectroscopy of graphene and related materials. 2024. https://doi.org/10.1016/B978-0-323-90800-9.00252-3.
13) Surekha G, Krishnaiah KV, Ravi N, Suvarna RP. FTIR, Raman and XRD analysis of graphene oxide films prepared by modified Hummers method. 2020. https://doi.org/10.1088/1742-6596/1495/1/012012.
14) Salehpoor M, Khoteeva NS, Grebenko AK, Luchkin SY, Raginov NI, Trepalin OR, et al. Graphene visualization on non-conductive substrates with standard mechanical channels of atomic force microscopy. *Emergent Materials*. 2025 Aug;8(6):5241–5249. https://doi.org/10.1007/s42247-025-01109-5.
15) Huo X, Sun L, Yang Z, Li J, Feng C, Zhang Z, et al. Mechanism and Quantitative Characterization of Wettability on Shale Surfaces: An Experimental Study Based on Atomic Force Microscopy (AFM). *Energies (Basel)*. 2023 Nov;16(22). https://doi.org/10.3390/en16227527.
16) Savulescu GC, Rücker M, Scanziani A, Pini R, Georgiadis A, Luckham PF. Atomic force microscopy for the characterization of pinning effects of seawater micro-droplets in n-decane on a calcite surface. *Journal of Colloid and Interface Science*. 2021 Jun;592:397–404. https://doi.org/10.1016/j.jcis.2021.02.070; https://pubmed.ncbi.nlm.nih.gov/33689984.
17) Kim E, Kim D, Kwak K, Nagata Y, Bonn M, Cho M. Wettability of graphene, water contact angle, and interfacial water structure. *Chem*. 2022;p. 1187–1200. https://doi.org/10.1016/j.chempr.2022.04.002.
18) Belyaeva LA, Tang C, Juurlink L, Schneider GF. Macroscopic and Microscopic Wettability of Graphene. *Langmuir*. 2021 Apr;37(14):4049–4055. https://doi.org/10.1021/acs.langmuir.0c02817; https://pubmed.ncbi.nlm.nih.gov/33651625.
19) Liu Z, Gao H, Wen S, Lin H, Chen X, Chen G. The influence of xylene content on the dispersion of graphene in aromatic petroleum resin by solution mixing. *Applied Surface Science*. 2021 Nov;567:150718. https://doi.org/10.1016/j.apsusc.2021.150718.
20) Narayan J, Bezborah K. Recent advances in the functionalization, substitutional doping and applications of graphene/graphene composite nanomaterials. *RSC Advances*. 2024;1:13413–13444. https://doi.org/10.1039/d3ra07072g.
21) Yamagishi T, Shibutani S, Suzuki H, Yamauchi S. Raman characterization of layer of graphene-like structures in 3d-transition metal-loaded charcoal by comparison with X-ray diffraction data. *Wood Science and Technology*. 2024 Jul;58(4):1451–1471. https://doi.org/10.1007/s00226-024-01563-0.
22) Low IM, Albetran HM, Degiorgio M. Structural Characterization of Commercial Graphite and Graphene Materials. *Journal of Nanotechnology and Nanomaterials*. 2020. Available from: https://www.scientificarchives.com/journal/journal-of-nanotechnology-and-nanomaterials.
23) Thaman HL, Li M, Rose JA, Narasimhan S, Xu X, Yeh CN, et al. Two-Stage Growth of Solid Electrolyte Interphase on Copper: Imaging and Quantification by Operando Atomic Force Microscopy. *ACS Nano*. 2025 Apr;19(12):11949–11960. https://doi.org/10.1021/acsnano.4c16418.
24) Chen G, Zhou H, Chen Y, Hu Z. Insight into the corrosion inhibition of sulfathiazole on the Cu surface by in-situ AFM observations and theoretical calculations. *Electrochimica Acta*. 2025 Nov;541:147330. https://doi.org/10.1016/j.electacta.2025.147330.
25) Ding Y, Li M, Guo Y, Dai R, Liu Z, Zhou D, et al. Characterization of crystallinity and graphene morphology on annealed copper foils: Enhancing electrical properties in copper/graphene composite. *Materials Characterization*. 2025 Oct;228:115366. https://doi.org/10.1016/j.matchar.2025.115366.
26) Lyu H, Xu X, Wang C, Li K, Jia X, Yan D, et al. Enhanced copper interconnect module based on flake graphene copper femtosecond laser processing. *Materials Letters*. 2025 Nov;399:139036. https://doi.org/10.1016/j.matlet.2025.139036.
27) Zhou K, Jia Y, Jia D, Wang J, Sun W, Wang Y, et al. Progress of highly conductive Graphene-reinforced Copper matrix composites: A review. *Journal of Materials Research and Technology*. 2024 Nov;33:7546–7571. https://doi.org/10.1016/j.jmrt.2024.11.076.
28) Liu W, Zhao X, Li H, Ding Y. Research Progress on the Preparation and Properties of Graphene–Copper Composites. *Metals, MDPI*. 2025. https://doi.org/10.3390/met15101117.

29) Song Y, Xiang L, Cheng X, Yang D, Vafai K. Normalization of wettability and heat transfer coefficient curve prediction model on biphilic surfaces. *Experimental Thermal and Fluid Science*. 2025 May;164:111427. https://doi.org/10.1016/j.expthermflusci.2025.111427.